Int J Thermophys (2007) 28:1342–1352
DOI 10.1007/s10765-007-0264-1

IR Radiometry Optical System View Factor and Its Application to Emissivity Investigations of Solid and Liquid Phases

J. Martan · N. Semmar · C. Boulmer-Leborgne

Received: 7 August 2006 / Accepted: 4 September 2007 / Published online: 3 October 2007

Abstract An optical system for fast IR radiometry designed for investigations of thin film thermal properties and pulsed laser melting was analyzed in this work. A methodology for determination of the view factor from calibration measurements was developed. The view factor (0.0255) of the optical system containing two paraboloid mirrors was determined experimentally from calibration measurements on pure metals and metallic alloys. The knowledge of the view factor was then applied to normal emissivity investigations at IR wavelengths. The emissivity of tungsten films prepared by magnetron sputtering was determined for different deposition conditions, varying between 0.036 and 0.071. Liquid phase emissivities of Cu, Mo, Ni, Si, Sn, Ti, and steel were also determined and were found to be higher than solid-state emissivities as predicted from the literature. A knowledge of the liquid-state emissivity of silicon enabled recalculation of the IR signal evolution to the temperature evolution, during and after a nanosecond laser pulse. This was not possible by use of the usual calibration because of silicon's semi-transparent behavior in the IR range (1–10 μm) in the solid-state phase.

Keywords Emissivity · Fast infrared radiometry · Liquid phase · Optical focusing system · View factor

J. Martan · N. Semmar · C. Boulmer-Leborgne
GREMI, CNRS/Université d'Orléans, 14, rue d'Issoudun, BP 6744, 45067 Orléans cedex 2, France

J. Martan (✉)
Department of Physics, University of West Bohemia, Univerzitní 22, Plzeň 30614, Czech Republic
e-mail: jmartan@kfy.zcu.cz

1 Introduction

Optical systems are widely used in non-contact temperature measurement systems based on infrared (IR) radiation detectors. They are used for attaining a sufficient level of the measured signal, and localizing the measurement area. In the present work, we analyze one of these optical systems in order to enable emissivity investigations using an IR radiometry system. During the analysis, the view factor of the optical focusing system is determined.

For determination of the absolute surface temperature evolution, it is necessary to know the optical properties of the investigated material, e.g., the spectral emissivity for opaque materials. This is an important limitation factor, which can be resolved by emissivity measurements, or calibration of the measurement system. Specific systems have been developed for minimizing the influence of the emissivity. They are based on two wavelength measurements [1], in situ emissivity monitoring [2], and the use of a reflective cavity [3].

Temperature measurement systems based on IR radiometry are widely used in the field of thermal property investigations. They consist mainly of an IR detector and an optical focusing system. The optical system can be a lens or a set of lenses, a system of two paraboloid mirrors or other concave mirrors, or an optical fiber. Most widely used are focusing mirrors (especially off-axis paraboloid mirrors) because their focal length is independent of wavelength. In the flash radiometry technique, a concave mirror [4] or ZnSe lens [5] was used. In photothermal infrared radiometry, two off-axis paraboloid mirrors [6] or an ellipsoidal mirror [7] has been applied. In the laser flash method, a silicon lens [8] or silica doublet lens [9] has been used.

In the present work, the selected optical system based on two paraboloid mirrors is analyzed in order to enable determination of the emissivity of unknown samples, and the liquid phase of different materials. The emissivity is determined from the IR detector response by the use of the view factor. A methodology for view factor determination from calibration measurements is demonstrated. Its value was experimentally determined for the chosen optical system. A theoretical calculation of the view factor is also presented.

Knowledge of the normal spectral emissivity at different temperatures, and for the liquid phase is rare, especially for IR wavelengths. Several studies have been published, but are usually focused on visible or near-infrared wavelengths. Spectral emissivities of metals, at high temperatures, in the solid phase have been investigated in [10] over the wavelength range from 1 to 16 μm. Spectral emissivities of pure molybdenum and tungsten in the solid phase at high temperatures, and in the liquid phase were investigated in [11] at three wavelengths from 680 to 1570 nm. Spectral emissivities of tin, zinc, aluminum, and silver at the melting temperature of solid and liquid phases were measured in [12] over the wavelength range from 1.5 μm to 5 μm. Spectral emissivities of solid and liquid iron, cobalt, and nickel at the melting point were determined in [13] over the wavelength range from 600 to 2000 nm. In the present work, the investigated emissivity is a weighted average for infrared wavelengths over the range of 2–12 μm with a peak at 10 μm.

2 Experimental System

The experimental system for fast IR radiometry (Fig. 1) was developed first for thermal property investigations of thin films [14]. The method is based on measurements of the change in the sample surface temperature with time induced by a short energetic laser pulse. The laser pulse duration was 5 ns (Nd:YAG laser at the fourth harmonic: 266 nm) or 27 ns (KrF laser). The infrared light emitted from the surface according to Planck's law is focused on the detector using two off-axis paraboloid mirrors. The first paraboloid mirror has an angle of 30° to the focal point, an effective focal length (EFL) of 81.5 mm, and a reflectivity of 98% (Coherent 43-9000-021). The second mirror has an angle of 90°, EFL of 76.2 mm, and a reflectivity of 90% (Melles Griot 02POA015). The IR detector is a liquid-nitrogen-cooled HgCdTe photovoltaic photodiode with a diameter of 0.25 mm and is sensitive in the spectral range from 2 to 12 μm (Kolmar Technologies KMP11-0,25-J1/100). The obtained signal is amplified with an internal preamplifier in a frequency range of dc to 100 MHz. In front of the detector is a germanium filter, which selects only wavelengths over 1.8 μm.

The investigated samples were pure metals, metallic alloys, and silicon in the "bulk" form: Au, Cu, Fe, Mo, Ni, Si, Sn, Ti, W, Zn, bronze, steel ČSN 15330, and stainless steel ČSN 17246. The chemical compositions of the samples can be found in previous reports [14–16]. The Si sample was a monocrystalline wafer with orientation (100) and a thickness of 575 μm, and a 50 μm thick surface layer doped with P. The metallic samples were mechanically polished. The investigated thin film samples were tungsten layers on iron substrates (W/Fe) prepared by magnetron sputtering from a pure tungsten target.

3 IR Detector Calibration

The surface temperature, during and after the laser pulse, was measured through the thermal radiation emitted from the sample surface. It is one of the few methods enabling surface temperature measurement on a nanosecond time scale.

In order to obtain the absolute temperature evolution on the surface of the measured sample, it is necessary to calibrate the IR detector response. The calibration is done for each sample because of the different emissivities of the investigated materials. In the calibration process, the samples are heated to different temperatures, and for each

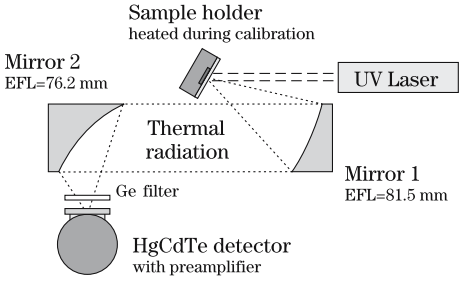

Fig. 1 Schematic representation of the experimental system of fast IR radiometry

temperature, a detector output voltage is measured. The voltage values plotted versus the sample temperature give the calibration curve.

A heated sample holder was used to obtain stabilized and homogeneous temperatures of the samples. It can be used from room temperature up to 500°C.

4 Optical System View Factor

In order to obtain a smooth calibration curve $U_1(T)$ for the complete temperature range, the measured points $U_m(T)$ are fitted by a theoretical calibration curve $U_0(T)$ using least squares. The fit is of the form,

$$U_1(T) = K\,U_0(T) + q, \tag{1}$$

where K is the calibration factor and q is an additive constant representing the room temperature radiation of the environment.

The theoretical calibration curve is obtained using

$$U_0(T) = r\,A \int R_n(\lambda) \frac{2\pi c^2 h \lambda^{-5}}{\exp(\frac{ch}{\lambda k T}) - 1} \mathrm{d}\lambda. \tag{2}$$

This equation is an integral of the emitted spectral power density, given by Planck's law [17], for all wavelengths, weighted by the normalized detector spectral responsivity curve $R_n(\lambda) = R(\lambda)/\max(R(\lambda))$, multiplied by the detector sensitive area A, and the peak detector–preamplifier responsivity $r = \max(R(\lambda))g$, where g is the preamplifier transimpedance gain. In Eq. 2, c is the speed of light, h is the Planck constant, λ is the wavelength, k is the Boltzmann constant, and T is the surface temperature. The integral is calculated numerically for wavelengths between 2 and 12 μm.

As the theoretical calibration curve is calculated based on assumptions of an ideal blackbody surface and no geometrical losses of the signal, the calibration factor K accounts for the emissivity ε of the real sample surface and the view factor f of the optical focusing system:

$$K = f\varepsilon. \tag{3}$$

The emissivity here is a weighted average of the normal spectral emissivity over wavelengths of the detector sensitivity (2–12 μm, with a peak at 10 μm). The view factor is a geometrical factor describing the portion of power irradiated from the sample surface in all directions that reaches the detector. It is a number describing the performance of the optical focusing system. An experimental value of the view factor is determined from Eq. 3, by using the experimental calibration curves for samples of different materials and their emissivities at IR wavelengths obtained from the literature (Table 1) for polished surfaces.

The theoretical value of the view factor is determined from the sizes, focal lengths, reflectivities R_{Au} and R_{Rh} of the paraboloid mirrors, transmissions of the Ge filter

Table 1 Normal spectral emissivities at IR wavelengths obtained from the literature [18–21]

Material	Au	Cu	Fe	Mo	Ni	Ti	W	Zn	Bronze	Steel
Emissivity (−)	0.02	0.02	0.05	0.04	0.03	0.1	0.04	0.03	0.02	0.07

T_{Ge}, the ZnSe detector entrance window T_{ZnSe}, and the atmosphere T_{at}:

$$f = f_a R_{Au} R_{Rh} T_{Ge} T_{ZnSe} T_{at}, \tag{4}$$

where f_a is the view factor between the second paraboloid mirror and the detector. The reason why the view factor of the second mirror is used, and not the first mirror, is described later in Sect. 6.1.

5 Emissivity Determination

The emissivity at IR wavelengths of an unknown sample is derived from Eq. 3 using the known view factor f and the calibration factor K determined by the usual calibration procedure. The resulting emissivity is the weighted average of the normal spectral emissivity over the wavelengths of the detector sensitivity.

The liquid-phase emissivity for IR wavelengths is derived from the plateau observed on the IR signal during the cooling phase. At the end of melting, the surface temperature remains at the melting temperature (slightly lower because of the melt undercooling—for more details, see Sect. 6.3). If the view factor of the optical system is known, the emissivity can be determined by Eq. 3. In this case, the calibration factor K is determined by a different procedure than for the solid phase. It is done by adjustment of the theoretical calibration curve to the two known points [initial temperature, zero signal] and [equilibrium melting temperature, voltage level of the plateau].

6 Results and Discussion

6.1 View Factor of the Optical System

Calibration of the IR surface temperature measurement system was carried out for all samples. An example of a calibration curve is shown in Fig. 2. The points represent the measured values, and the lines represent the fitted theoretical curves. The calibration factors range from 5.3×10^{-4} for copper to 2.67×10^{-3} for the titanium sample.

The temperature measurement system sensitivity is obtained by differentiation of the calibration curves. It is different for different samples. The sensitivity is dependent on the surface temperature and emissivity of the measured sample. The lowest sensitivity was found for the copper sample: 8–53 $\mu V \cdot K^{-1}$, and highest for the titanium sample: 29–200 $\mu V \cdot K^{-1}$, for the temperature range of 25–350°C.

The optical system view factor was determined from Eq. 3, by using calibration curves and literature values of emissivity for the used samples. A line fit for the view

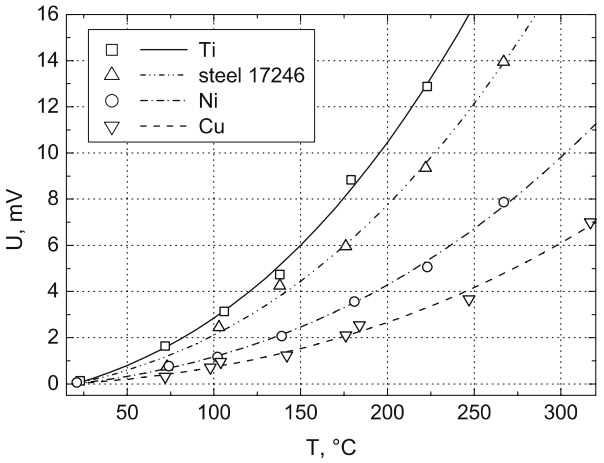

Fig. 2 Selected calibration curves—for Cu, Ni, Ti, and stainless steel 17246 samples

factor shown in Fig. 3 gives $f = 0.0255$. This view factor is a global factor for the complete optical system, and also takes into consideration the reflectivities of the paraboloid mirrors, and transmissions of the Ge filter and the ZnSe detector window.

The theoretical prediction using Eq. 4 gives

$$f = f_{\mathrm{a}} R_{\mathrm{Au}} R_{Rh} T_{\mathrm{Ge}} T_{\mathrm{ZnSe}} T_{\mathrm{at}} = 0.098 \times 0.98 \times 0.9 \times 0.4 \times 0.95 \times 0.95 = 0.0311 \tag{5}$$

where f_{a}, the view factor between the second paraboloid mirror and the detector, was calculated from the two parallel disks configuration with a radius of the mirror $r_{\mathrm{a}} = 25\,\mathrm{mm}$, a radius of the detector $r_{\mathrm{b}} = 0.125\,\mathrm{mm}$, and their relative distance

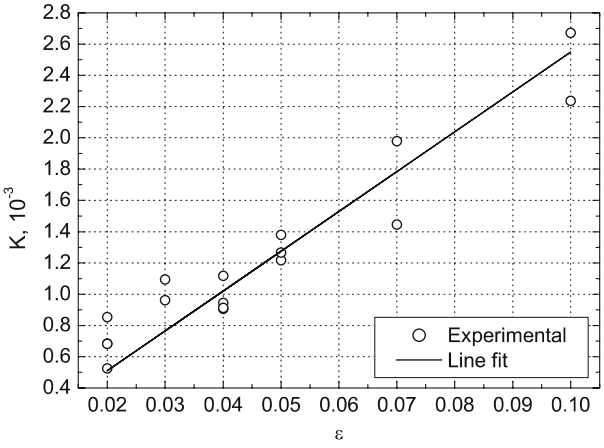

Fig. 3 Calibration factor plot versus the sample surface emissivity with a line fit for the view factor

$c = 76.2$ mm. The germanium filter was uncoated; thus, its relatively low transmissivity decreased the performance of the optical system. The theoretically predicted view factor is slightly higher than the experimental value (0.0255).

During analysis and design of the optical system, it was found numerically [15] and later experimentally with different mirrors, that the power density arriving the detector is dependent only on the effective focal length (EFL) of the second mirror and not on that of the first mirror near the sample—for the case of homogeneous temperature distribution on the sample surface. The EFL of the first mirror determines only the size of the spot on the sample, from which the radiation is detected. For obtaining the highest signal at the detector, the second mirror (near the detector) should be chosen with the shortest EFL possible. The only limitation is the geometrical arrangement of the mirror near the Dewar for liquid-nitrogen cooling of the detector.

6.2 Emissivity of Tungsten Thin Films

Using the present system, the thermal properties of tungsten thin films were investigated [22]. Four samples were prepared under two different deposition conditions of magnetron sputtering (different argon pressures of 1 and 0.28 Pa), and with different thicknesses (0.5 and 1.3 μm). The calibration was performed for the four samples. The experimental and fitted theoretical calibration curves are shown in Fig. 4. The calibration curves show different optical behavior for samples prepared under different deposition process parameters. The films deposited under the same conditions have the same calibration curves for both film thicknesses. The calibration factors are 1.82×10^{-3} for JM1 and JM2 (higher pressure), and 9.1×10^{-4} for JM3 and JM4 (lower pressure). Sample surface IR emissivities calculated using the experimentally determined optical system view factor are: 0.071 for the samples JM1 and JM2, and 0.036 for the samples JM3 and JM4. The emissivity of bulk tungsten is reported to be between 0.017 and 0.040 [18–21]. The emissivity 0.036 for the films JM3 and

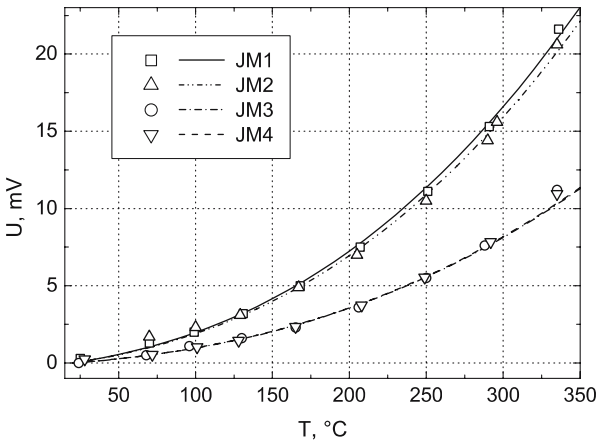

Fig. 4 Calibration curves for the JM1-4 samples of W films on Fe substrates

JM4 lies between 0.017 and 0.040, and can thus be taken as the bulk value. The films prepared at higher pressures have a higher emissivity than those at lower pressures. It is probably caused by the presence of more crystallographic defects in the films JM1 and JM2, or the different morphological structures of the film's surface.

6.3 Liquid-phase Emissivity

The present surface temperature measurement system was also used in investigations of nanosecond laser melting [16]. During cooling after the laser pulse, a solidification plateau appears at the end of the solidification of the liquid phase. An example of the IR signal during and after laser melting is shown in Fig. 5. At the end of solidification, the surface temperature is almost constant and close to the equilibrium melting temperature (as predicted in [23]). From this information the calibration factor for the liquid phase can be determined, and with a knowledge of the view factor, the liquid-phase emissivity can be calculated. A peak after the plateau, as shown in Fig. 5, is specific for silicon and not present for metallic samples. It is caused by changes in the optical behavior of silicon with phase change as described in [16]. Oscillations at the beginning of the plateau are perturbations produced by the IR detector after a fast change in the IR signal.

Liquid-phase emissivities were determined by this method for the metallic and silicon samples. The resulting emissivities are shown in Table 2, accompanied with the voltage levels of the solidification plateau and equilibrium melting temperatures.

The measured liquid-phase emissivities are higher than solid-phase emissivities found in the literature, which is in accordance with theoretical predictions [18]. The lowest emissivity was found for the copper sample, which was very close to the solid-phase emissivity. The highest value was observed for the titanium liquid phase. The emissivity of the two steel samples was found to be almost the same. Using the

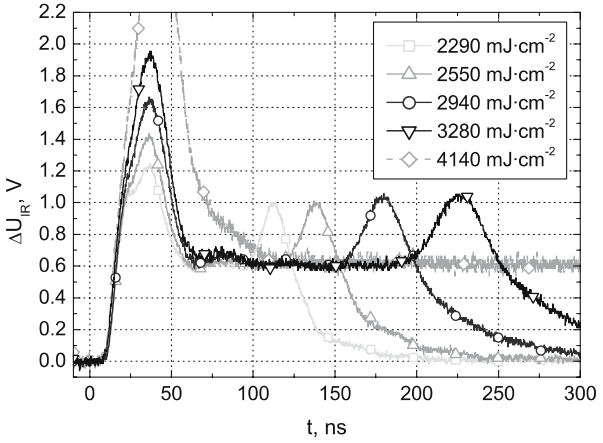

Fig. 5 Si sample IR signal including surface melting induced by the KrF laser for different incident laser energy densities

Table 2 Measured liquid-phase normal spectral emissivities at IR wavelengths

Sample	U_{IR} (V)	T_m (°C)	ε_l (−)
Si	0.61	1412	0.086
Mo	2.2	2623	0.093
Ni	0.65	1453	0.087
Cu	0.11	1085	0.028
Sn	0.01	232	0.075
Ti	1.7	1670	0.17
Ti β phase	0.26	882	0.104
Steel 15330	0.86	1500	0.107
Steel 15330 γ phase	0.095	790	0.049
Stainless steel 17246	0.875	1500	0.109

U_{IR} is the voltage level of the solidification plateau, T_m is the equilibrium melting temperature obtained from the literature [18,24–26], and ε_l is the liquid-phase emissivity

obtained emissivity values, the IR radiation evolution during the melting phase can be recalculated to the surface temperature without any calibration, which would be very difficult.

The melted silicon sample showed an emissivity comparable to the metallic samples. Silicon is semitransparent for IR wavelengths in the solid state, but in the liquid state it behaves like metals—an opaque surface with low emissivity. The solid-state transparency of Si did not allow the use of usual calibration procedure with steady-state heating for recalculation of the IR signal at the surface temperature. In the liquid phase the surface temperature evolution can be recalculated by using the obtained liquid-phase emissivity. The recalculated surface temperature evolutions of melted silicon are shown in Fig. 6.

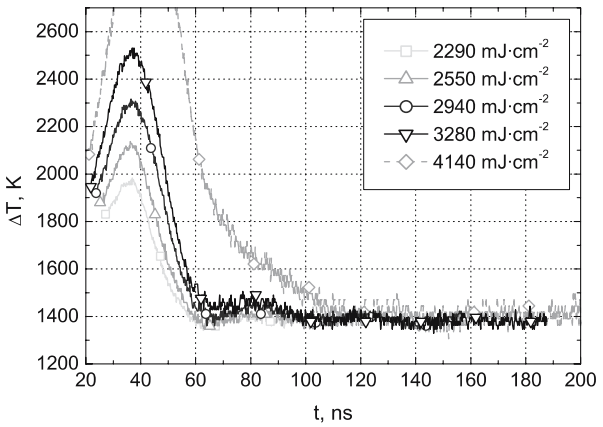

Fig. 6 Si sample liquid-phase temperature evolution induced by the KrF laser. Curves were recalculated from IR detector voltage response using emissivity determined from knowledge of the optical system view factor

7 Conclusion

An optical system used in a fast non-contact surface temperature measurement system based on IR radiometry was analyzed. It contains two paraboloid mirrors. A methodology for determination of the view factor from calibration measurements was developed. The optical system view factor was calculated from the set of calibration curves for known metallic samples and literature values of their emissivity. The value of the view factor is 0.0255. A theoretical value of the view factor was found to be in agreement with the measured result.

For improvement of the IR radiometry system, an anti-reflection coated Ge filter should be used, and a second paraboloid mirror with a shorter distance x of the detector to the mirror (off-axis angle of 90°) can be used.

Using the determined view factor of the optical system, the IR emissivity of tungsten thin films was determined. Its value is 0.071 for higher-pressure deposition conditions and 0.036 at lower pressures.

The knowledge of the view factor was further applied to IR emissivity investigations of melted materials. Materials are melted by a nanosecond pulsed laser, and the emissivity of the liquid phase is identified from the plateau on the IR signal at the end of solidification. This emissivity can then be used for surface temperature determination from the IR signal throughout the existence of the liquid phase during and after the laser pulse. The liquid-phase emissivity was identified for different metallic samples and silicon. For the silicon sample, the liquid-phase temperatures during and after the laser pulse were recalculated, which was not possible by the use of usual calibration because of its semi-transparency in the solid state.

Acknowledgment The work has been supported by research project MSM4977751302 of the Ministry of Education of the Czech Republic.

References

1. L. Tong, Y. Shen, L. Ye, Sensors Actuators **75**, 35 (1999)
2. M. Hatano, S. Moon, M. Lee, K. Suzuki, C.P. Grigoropoulos, J. Appl. Phys. **87**, 36 (2000)
3. J.C. Krapez, C. Belanger, P. Cielo, Meas. Sci. Technol. **1**, 857 (1990)
4. W. P. Leung, A.C. Tam, J. Appl. Phys. **56**, 153 (1984)
5. W.P. Leung, A.C. Tam, J. Appl. Phys. **63**, 4505 (1988)
6. S. Paoloni, L. Nicolaides, A. Mandelis, Rev. Sci. Instrum. **71**, 2445 (2000)
7. B. Zhang, R.E. Imhof, Appl. Phys. A-Mater. Sci. Process. **62**, 323 (1996)
8. H. Ohta, H. Shibata, Y. Waseda, Rev. Sci. Instrum. **60**, 317 (1989)
9. D. Demange, P. Beauchene, M. Bejet, R. Casulieras, Rev. Gen. Therm. **36**, 755 (1997)
10. W. Bauer, H. Oertel, M. Rink, presented at the 15th Symposium on Thermophysics Properties (Boulder, Colorado, June 22–27, 2003)
11. C. Cagran, G. Pottlacher, M. Rink, W. Bauer, Int. J. Thermophys. **26**, 1001 (2005)
12. K. Boboridis, A. Seifter, A.W. Obst, D. Basak, Int. J. Thermophys. **25**, 1187 (2004)
13. H. Watanabe, M. Susa, H. Fukuyama, K. Nagata, Int. J. Thermophys. **24**, 473 (2003)
14. J. Martan, N. Semmar, C. Leborgne, E. Le Menn, J. Mathias, Appl. Surf. Sci. **247**, 57 (2005)
15. J. Martan, *Thermo-kinetic model of laser-material interaction in the form of criteria equations* (Ph.D. thesis, Faculty of Applied Sciences, University of West Bohemia in Plzen, Czech Republic, Ecole Polytechnique, University of Orleans, France, 2005)
16. J. Martan, O. Cibulka, N. Semmar, Appl. Surf. Sci. **253**, 1170 (2006)
17. G. Gaussorgues, *Infrared Thermography* (Chapman & Hall, London, 1994)

18. M. von Almen, *Laser-Beam Interactions with Materials, Springer Series in Material Sciences* (Springer Verlag, Berlin, Heidelberg, 1987), pp. 201–204
19. Y.S. Touloukian, D.P. DeWitt, *Thermophysical Properties of Matter, Vol 7, Thermal Radiative Properties – Metallic Elements and Alloys* (Plenum, New York, 1970)
20. D.R. Lide (ed.), *CRC Handbook of Chemistry and Physics*, 79th edn. (CRC Press, Boca Raton, Florida, 1999), pp. 12-127–12-149
21. H.C. Hottel, A.F. Sarofim, *Radiative Transfer* (MacGraw-Hill, New York, 1967), p. 155
22. J. Martan, N. Semmar, C. Leborgne, P. Plantin, E. Le Menn, Nanoscale Microscale Thermophys. Eng. **10**, 333 (2006)
23. V.N. Tokarev, A.F.H. Kaplan, J. Appl. Phys. **86**, 2836 (1999)
24. H. Baker, in *ASM Handbook, Vol 3*, *Alloy Phase Diagrams* (ASM Int., Materials Park, Ohio, 1999)
25. Web Elements Material Properties Database, http://www.webelements.com
26. J. Jech, *Heat Treatment of Steel (Czech)* (SNTL, Praha, 1983)